Aerodynamic Effects of Probe-Induced Flow Separation on Bluff Bodies at Transonic Mach Numbers

Bruce F. Haupt*
U.S. Air Force Armament Laboratory, Eglin Air Force Base, Florida
and
Keith Koenig†
Mississippi State University, Mississippi State, Mississippi

An experimental investigation using probe-induced flow separation devices to reduce transonic blunt-body drag has been conducted. Particularly examined were blunt axisymmetric mainbodies with axially aligned cylindrical probes extended ahead. The experiments were performed in a ballistic facility, and the data obtained include drag coefficients and shadowgraphs of the flowfield. Drag reductions of 25% were observed over the Mach number range 0.85–1.25. Flow visualization reveals a distinct difference in the manner in which the flow reattaches to the mainbody for low- and high-drag geometries. The flowfield also exhibited modes resembling open- and closed-cavity flows, depending primarily on the probe length. Large-scale flow oscillations were observed for both low- and high-drag cases. This work clearly demonstrates the possibility for transonic drag reductions using cylindrical probes and provides useful information on more fundamental questions concerning transonic flow separation and reattachment.

Nomenclature

C_{D_0} = zero angle-of-attack drag coefficient
C_{P_0} = stagnation pressure coefficient
d_1, d_2 = probe and mainbody diameters, respectively
ℓ = probe length
ℓ/d_1 = probe fineness ratio
M = flight Mach number

Introduction

THE usual practice in the aerodynamic design of fuselage-like bodies is to elongate and streamline the forebody to minimize the forebody pressure drag. Conflicting situations do arise, however, where a more blunt-nose shape is necessary and yet low drag is still desired. One scheme for resolving this dilemma involves effectively streamlining the blunt nose by the use of an aerodynamic device positioned and shaped so as to induce flow separation ahead of the nose. The dynamic pressure level within the separated zone is sufficiently depressed, relative to the flow without the device, that the net forebody pressure drag (which includes the drag of the device) is decreased. This approach to drag reduction has been successfully applied in several practical cases, most notably in the use of cab-mounted air deflectors on tractor-trailer trucks[1] and in the use of a nose spike on the Trident submarine-launched ballistic missile.[2]

Both the tractor-trailer (with or without an air deflector) and the missile with a nose spike share several geometric and fluid mechanical features found in less complex situations such as flow past cavities, forward-facing steps, probes, and other multiple blunt bodies. Apart from the numerous studies concerning trucks and specific missiles, abundant data are available regarding the fundamental fluid mechanical behavior of steps, cavities, and multiple blunt bodies in both low Mach number[3–7] and supersonic and hypersonic[8–16] streams. Studies such as these have provided fundamental insight and a data base for aerodynamic design using flow separation. Additionally, they have clearly demonstrated that induced flow separation can be effectively exploited to decrease forebody drag.

In contrast to the preceding examples, there appear to be few (if any) intentional applications of induced flow separation for transonic drag reduction of blunt bodies. Furthermore, transonic flow past related geometries (probes, forward-facing steps, cavities) seems to be the subject of only a limited number of studies[17–20] in the open literature. Among the few studies available, the most interesting is the work of Spooner,[19] who observed large reductions in the transonic drag of a flat-faced artillery shell when a flat-faced cylindrical probe was extended ahead. Unfortunately, no other work is known to the authors that can serve to corroborate these results directly. Nevertheless, in view of what is known for other Mach number regimes, it would seem plausible, as Spooner observed, that induced flow separation devices can significantly reduce the transonic drag of blunt-nosed bodies. The ultimate reductions possible and the nature of the devices required to obtain these reductions are, however, not at all obvious.

The present investigation has been undertaken in response to the results reported in Ref. 19 for transonic flow and the experience gained from the extensive work done at other Mach numbers. The purpose of this study is to explore the potential for transonic drag reduction of a blunt-nosed, axisymmetric body using probe-induced flow separation and to provide some insight into the associated fluid mechanical phenomena. The results of this study are encouraging and should serve as a starting point for more comprehensive investigations and as a basis for practical applications. The following paragraphs include a description of the ballistics range test facilities, test conditions, and blunt bodies, followed by a detailed discussion of the quantitative measurements of the drag coefficients and qualitative observations of the flowfield.

Experimental Details

Facilities and Test Conditions

Free-flight subscale ballistics experiments were performed in the Aeroballistic Research Facility[21] at the U.S. Air Force Armament Laboratory. The working section is 207 m in length and contains 50 calibrated orthogonal shadowgraph stations. All the bodies were launched at atmospheric pressure conditions and at Mach numbers nominally between 0.75 and 1.25,

Presented as Paper 85-0103 at the AIAA 23rd Aerospace Sciences Meeting, Reno, NV, Jan. 14–17, 1985; received March 17, 1986; revision received Aug. 8, 1986.

*Capt., USAF, Assistant Chief, Aerodynamics Branch. Member AIAA.
†Associate Professor, Department of Aerospace Engineering. Member AIAA.

with corresponding Reynolds numbers based on mainbody diameter d_2 of 6.0×10^5 to 8.5×10^5. The bodies were fired from a smooth-bore 40-mm-i.d. launcher using a sabot that consisted of a two-component bore rider on the nose and a pusher plug, which acted as a gas seal, at the base. The segments of the sabot were aerodynamically stripped during launch.

The data obtained include zero angle-of-attack total drag coefficients C_{D_0} and shadowgraphs of the flowfield. The measuring capability of the facility is approximately 0.08 deg in orientation and 0.03 cm in position.[21] The trajectory data obtained from the shadowgraphs were reduced to coefficients using linear theory analysis and a six-degree-of-freedom numerical integration technique known as the maximum likelihood method.[22] All coefficients are based on freestream values and the mainbody diameter $d_2 = 0.372$ m. The experimental uncertainty for the coefficients is estimated to be $\pm 2\%$. The shadowgraphs shown in Figs. 7–12 were produced using a spark gap unit and x-ray film. The rise time of the spark is approximately 0.1 μs, with a total duration of 0.2–0.3 μs.

Blunt Bodies

The eleven blunt bodies considered in this investigation are displayed in Fig. 1. Three classes of mainbody shapes were considered. Configurations 1 and 2 represent the most basic flat-faced circular cylinder mainbody, plane and with an axially aligned cylindrical probe, respectively. Configurations 3–10 depict moderately blunt rounded mainbodies with axially aligned cylindrical probes. Configuration 3 is the reference configuration for this study and was selected because of its similarity to conventional aircraft stores with moderately blunt rounded mainbodies. The front of the probe for configuration 3 has a rounded corner with a radius of 0.08 d_2. All the other cylindrical probes have flat faces with no rounding. This was done to facilitate comparison with data from other flat-faced cylindrical body investigations.[8, 9, 19, 23] Configuration 11 is a simple hemispherical-nosed body without a probe. The various forebodies were constructed of brass or copper to achieve the desired c.g. location, whereas the remainder of the configuration, body and fins, were machined from aluminum. In the discussion of the results, the exposed length of the probe will be denoted by ℓ, the diameter of the probe by d_1, and the mainbody diameter by d_2. The length-to-mainbody-diameter ratio ℓ/d_2 and the probe fineness ratio ℓ/d_1 will be used extensively as parameters of comparison between configurations.

Measurements of the Drag Coefficient

To illustrate the essential characteristics of induced flow separation techniques, Fig. 2 displays the effect of a blunt probe on flat-faced axisymmetric bodies. Results for configurations 1 and 2 from the present study appear together with the results for configuration E3 from Ref. 19. The freestream stagnation pressure coefficient and the results for configuration 5 are also presented as references. The measurements from Ref. 19 are total drag coefficients obtained in wind-tunnel tests and adjusted to freestream static pressure at the base.

Without a probe, the Spooner[19] body has an exceptionally large drag coefficient, with a value essentially the same as the stagnation pressure coefficient over the Mach number range shown. When a probe is added, the drag is dramatically reduced, here by a factor of nearly 3. Note, however, that the transonic drag rise is greater for the body with the probe; that is, the percentage drag increase with increasing Mach number is greater for the probe/body configuration. Configuration 1 from the present work has a completely flat face and a corresponding high drag coefficient, although not as high as the Spooner body without a probe. Adding a probe of approximately the same relative size as that used in Ref. 19, to give configuration 2, produces a significant drag reduction which, however, on both an absolute and a percentage basis, is not quite as large as the reduction for the Spooner body. Differences in the present results and those of Ref. 19 are presumably a consequence of differences in the experimental circumstances of the two investigations. In any case, it is apparent that a probe can produce substantial drag reductions through the transonic regime, at least for flat-faced bodies. Included in Fig. 2 are the results for configuration 5 to illustrate that further decreases in drag are possible when the mainbody face corners are rounded. As a final comment on Fig. 2, it is important to note that only one probe was used in Ref. 19 and for the flat-faced body tests of the present work. Consequently, the results in Fig. 2 are only representative; greater drag reductions may be possible for a different probe length and diameter.

The configurations with a rounded mainbody face can be grouped as to constant probe length or constant probe diameter, and Figs. 3–5 present the variation of drag coefficient with Mach number according to such groupings. Four probes with the same diameter ratio as the reference body (configuration 3, $d_1/d_2 = 0.368$) were investigated in this study, and the results of these configurations appear in Fig. 3. In this figure, the behavior of the various bodies begins to become noticeably different near $M = 0.85$, with the longer probes having less drag as the Mach number increases. From approximately $M = 0.85$ upward to the highest Mach number tested, configurations 5 and

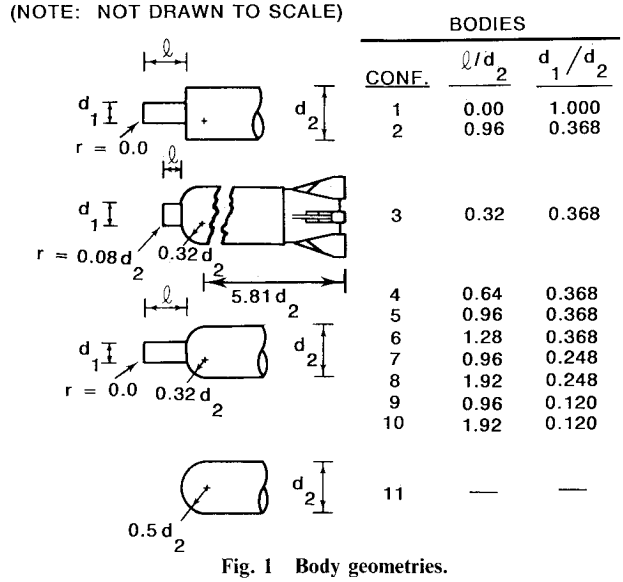

CONF.	ℓ/d_2	d_1/d_2
1	0.00	1.000
2	0.96	0.368
3	0.32	0.368
4	0.64	0.368
5	0.96	0.368
6	1.28	0.368
7	0.96	0.248
8	1.92	0.248
9	0.96	0.120
10	1.92	0.120
11	—	—

BODIES

Fig. 1 Body geometries.

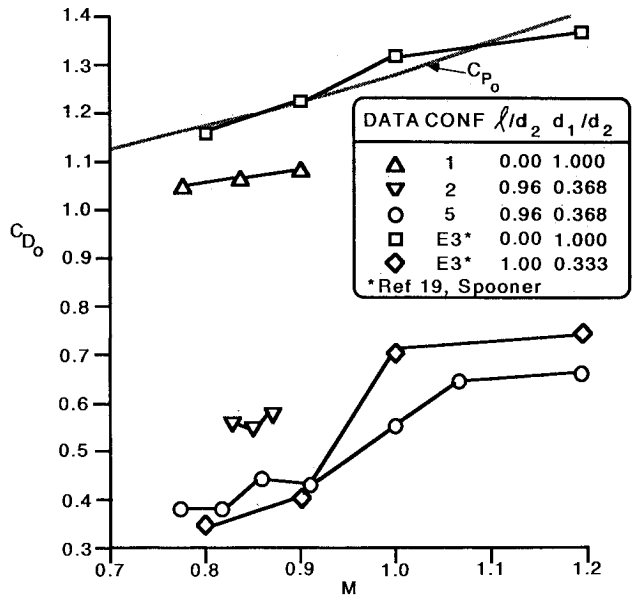

Fig. 2 Influence of a probe on the transonic drag of flat-faced axisymmetric bodies.

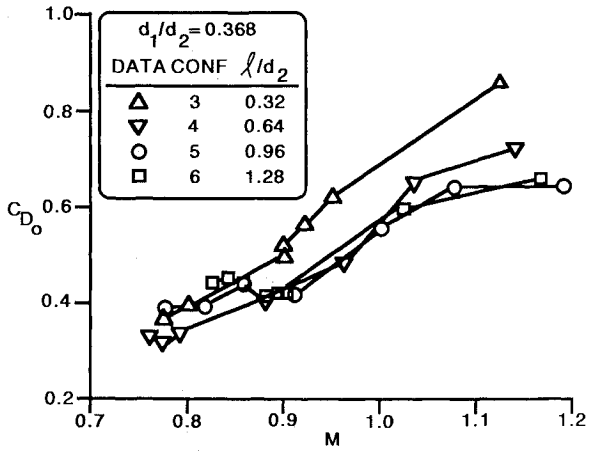

Fig. 3 Influence of probe length on transonic drag, $d_1/d_2 = 0.368$.

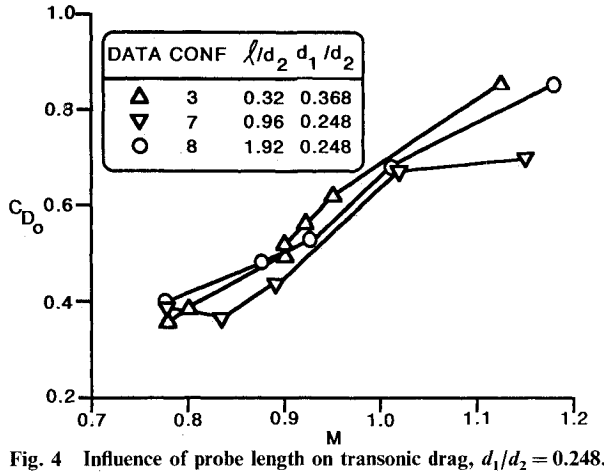

Fig. 4 Influence of probe length on transonic drag, $d_1/d_2 = 0.248$.

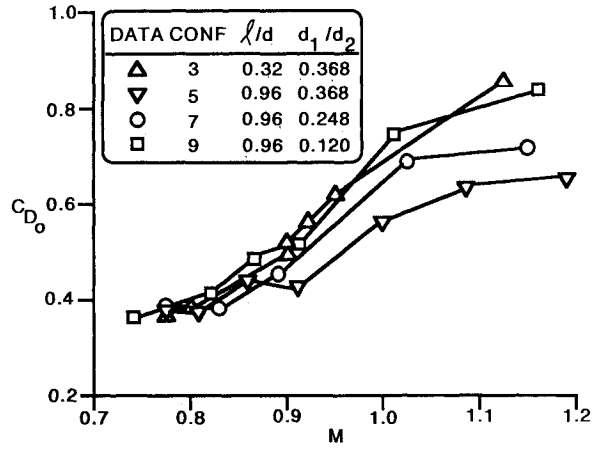

Fig. 5 Influence of probe diameter on transonic drag, $\ell/d_2 = 0.96$.

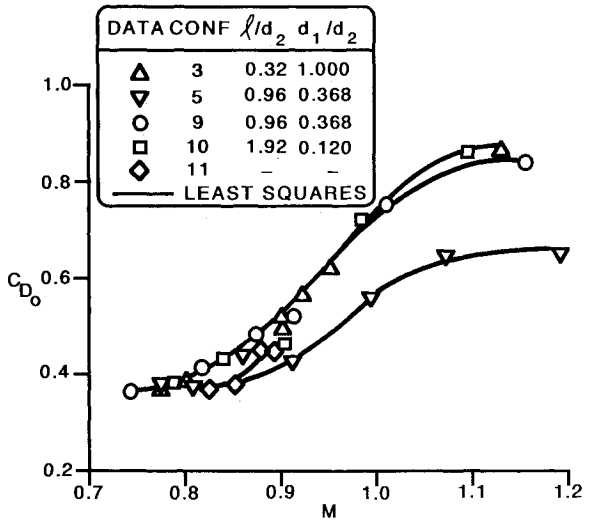

Fig. 6 Representative examples of the influence of probe geometry on transonic drag.

6 have only about 75% of the reference-body drag. It is important to note here that the drag reduction due to the probe begins at a subsonic freestream Mach number. This is in contrast to the results for the Trident missile,[2] where no subsonic drag reduction was observed. The spike used for the subsonic tests in Ref. 2 was extremely slender, $d_1/d_2 = 0.05$, and presumably did not produce sufficient separation upstream of the mainbody to reduce the drag.

In Fig. 4, the drag coefficient is shown for two configurations with a smaller-diameter probe ($d_1/d_2 = 0.248$), along with the reference body. For the short probe of the reference body, it is perhaps reasonable to assume that a change in probe diameter from $d_1/d_2 = 0.368$ to 0.248 will not have an overly large influence on the drag coefficient. If this is assumed, Fig. 4 indicates that, for given M and d_1/d_2, there is an optimum probe length at which the drag is minimum. With this in mind, we return to Fig. 3; configurations 5 and 6 have the same drag and therefore presumably bracket the optimum probe length for this particular probe diameter. That is, the optimum length is between $\ell/d_2 = 0.96$ and 1.28 for $d_1/d_2 = 0.368$. Figure 4 does not provide enough information to identify the optimum length for the smaller probe diameter although there clearly must be an optimum.

An example of the influence of probe diameter for fixed probe length is given in Fig. 5 for three probes with nondimensional length $\ell/d_2 = 0.96$ (again with configuration 3 as a reference). At this length, increasing the probe diameter decreases the drag for Mach numbers greater than approximately 0.85. This trend cannot continue indefinitely, however, since at $d_1/d_2 = 1.0$, the configuration becomes simply a flat-faced cylinder for which the drag is much higher than even that of the reference body. Thus, there must also be an optimum probe diameter yielding a minimum drag, given the Mach number and probe length.

A summary of the more important results obtained from the drag measurements is presented in Fig. 6. The configurations selected for this figure emphasize the influence that probe length and diameter have on the overall drag. Configurations 3 and 10, although they have quite different probes (probe fineness ratio, $\ell/d_1 = 0.87$ and 16.0, respectively), have essentially identical drag coefficients. Clearly there must be an optimum configuration, which has a length and diameter intermediate to those of configurations 3 and 10. Shortening the probe of configuration 10 to give configuration 9 does reduce the drag; an increase in diameter to give configuration 5 produces further drag reduction. Notice that configuration 5 has a lower drag level than a hemispherical-nosed body (configuration 11). Also, notice that the drag reduction with configuration 5 begins near Mach 0.85; the use of a probe as a drag-reduction device is effective below Mach 1 as well as for supersonic speeds.

As a side note to Fig. 6, the smooth, solid curves on this figure were obtained from a least-squares curve fit to the expression $C_{D_0} = a + b \tanh(bM + c) + d$, where a, b, c, and d are constants (for a given body) determined by the curve fit. This expression, although purely empirical, satisfactorily describes the variation of drag coefficient with Mach number in the transonic regime. It is limited, of course, to monotonic functions $C_{D_0}(M)$ but otherwise appears to be generally valid. Since there are no well-established and general descriptions of transonic drag, this expression serves as a useful tool for interpolations and comparisons.

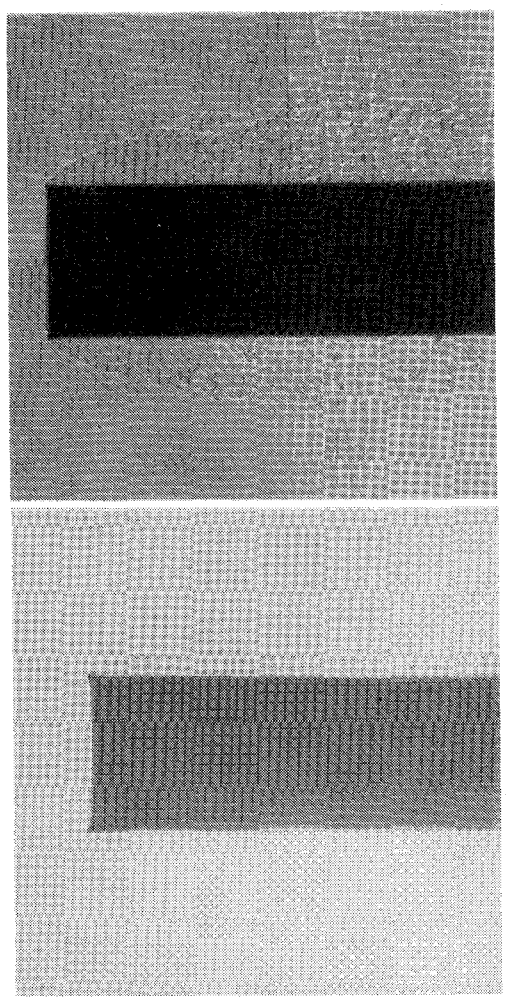

Fig. 7 Basic flowfield for a flat-faced body, configuration 1, $\ell/d_2 = 0.0$, $d_1/d_2 = 1.0$: *a*) $M = 0.86$, $C_{D_0} = 1.05$; b) $M = 1.00$, $C_{D_0} = 1.14$.

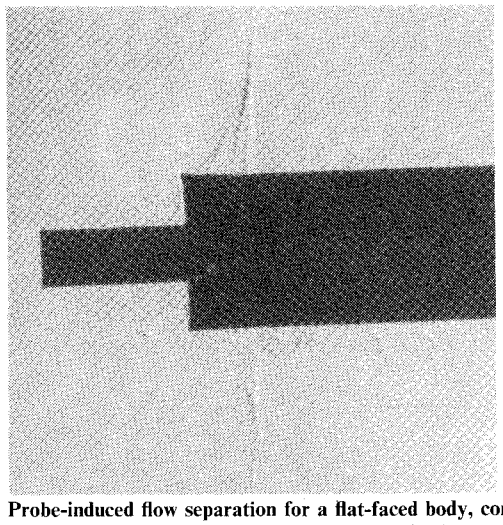

Fig. 8 Probe-induced flow separation for a flat-faced body, configuration 2, $\ell/d_2 = 0.96$, $d_1/d_2 = 0.368$, $M = 0.87$, $C_{D_0} = 0.56$.

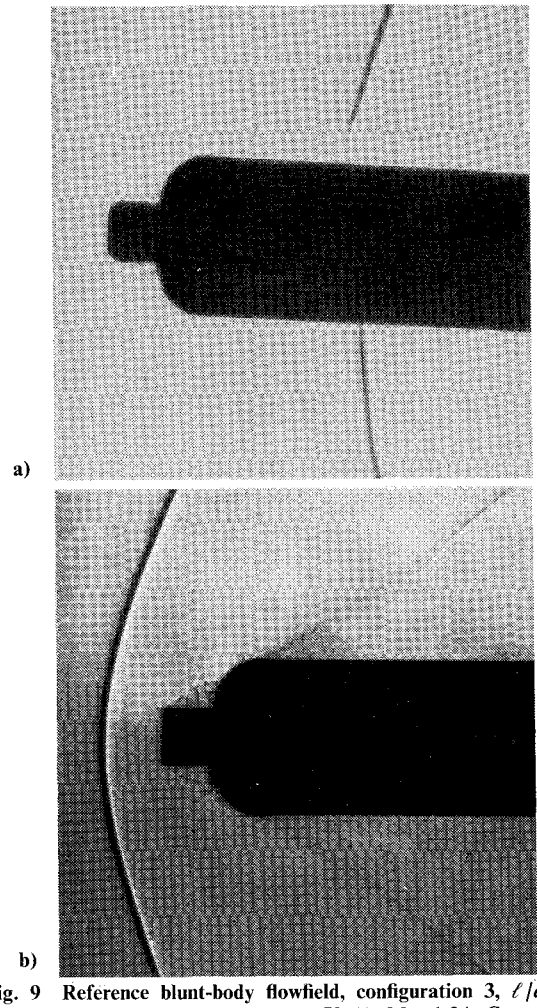

Fig. 9 Reference blunt-body flowfield, configuration 3, $\ell/d_2 = 0.32$, $d_1/d_2 = 0.368$: a) $M = 0.94$, $C_{D_0} = 0.58$; b) $M = 1.24$, $C_{D_0} = 0.93$.

Observations from the Flow Visualization

Basic Flowfield

The most basic of forebody shapes is perhaps a plane or flat face. The flowfield for such a forebody is depicted in Fig. 7 for subsonic ($M = 0.86$) and sonic Mach numbers. For the subsonic case (Fig. 7a), the extensive region of separated and turbulent flow downstream of the face accompanied by a system of weak normal shock waves at roughly 2 diameters downstream in the reattachment zone is quite visible. The large region of separation and turbulence is indicative of the high forebody drag, the drag coefficient being 1.05 for this situation. At a flight Mach number of 1 (Fig. 7b), the flowfield is significantly different. The separated region has a much smaller lateral extent, and the reattachment shock system is now a system of coalescing compression waves, which form a single, well-defined oblique shock. The drag coefficient has increased as a consequence of the natural increase in stagnation pressure coefficient with Mach number, as demonstrated in Fig. 2.

As previously observed in Fig. 2, if a probe is extended in front of the flat-faced forebody, there is a significant reduction in the drag coefficient. Figure 8 shows the flat-faced cylinder with a probe for which the drag coefficient is barely half that without the probe. The separated and turbulent region downstream of the face is smaller here, and the probe has effectively streamlined the forebody. Notice that the shock system has moved forward and that a stronger, more clearly defined normal shock is apparent. Also visible are spherical Mach waves produced by the turbulent fluctuations and propagating away from the body. Many of the waves appear to originate at the corner of the mainbody face. These may be the result of large-scale oscillations of the free shear layer interacting with the mainbody face corner.[24]

The primary emphasis of the present investigation concerns geometrical variations from the reference body, configuration 3. The flowfield for the reference body at $M = 0.94$ is shown in Fig. 9a. Visible in this shadowgraph are the separated flowfield from the probe face that impinges on the mainbody face, expansion waves radiating from the mainbody corners, a system of coalescing compression waves terminating in a normal shock, and a turbulent boundary layer originating at the foot

of the shock. The parallel lines aft of the shock are caused by light rays intersecting portions of the normal shock (which is actually slightly curved) that are radially far removed from the body. This same body at $M = 1.24$ is seen in Fig. 9b. Here the strong bow shock is apparent, and an oblique shock replaces the subsonic case normal shock on the body sides. The separated flowfield from the probe reattaches to the mainbody face as in the subsonic case, and the drag coefficient, 0.93, is quite high.

A variety of probes were investigated for this mainbody. The probe giving the greatest transonic drag reduction was configuration 5. Figure 10 presents the flowfield for this body at essentially the same Mach numbers as are shown for configuration 3 in Fig. 9. Most of the flowfield details for these two forebody shapes are qualitatively similar, except for one especially significant difference. For configuration 5, the probe separation appears to reattach almost tangentially to the mainbody side rather than impacting the face, which occurs for configuration 3. In careful studies done in an incompressible freestream,[6,7] a flow separation device (a thin disk) ahead of a flat-faced cylinder was found to produce minimum forebody drag when the separation reattached smoothly (tangentially) onto the cylinder sides. For this situation, the pressures on the cylinder face and turbulent shear stresses in the separated shear layer were both quite small, thus leading to low drag. Presumably, a similar phenomenon is occurring for transonic flow with a probe. Low forebody drag is a consequence when the probe induces separation in such a way that the reattachment is roughly tangential to the mainbody sides.

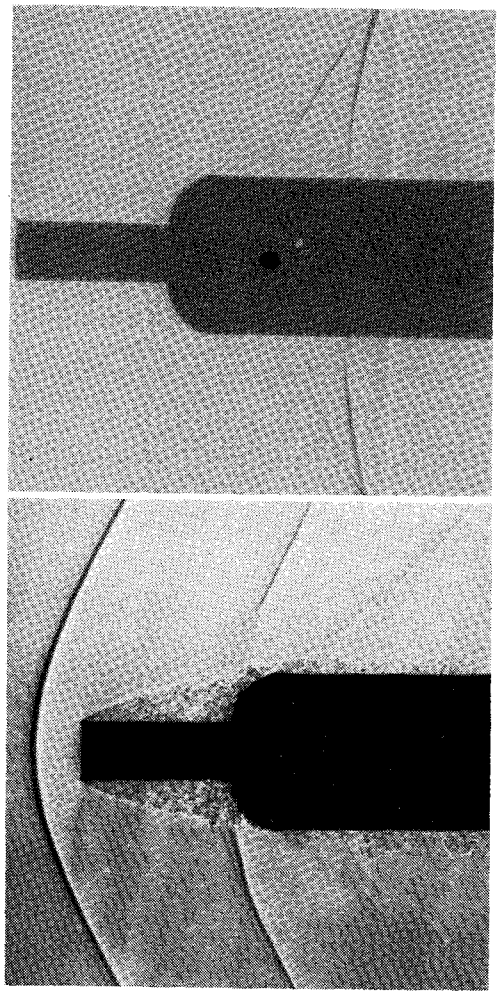

Fig. 10 Transonic probe-induced flow separation, configuration 5, $\ell/d_2 = 0.96$, $d_1/d_2 = 0.368$: a) $M = 0.95$, $C_{D_0} = 0.47$; b) $M = 1.27$, $C_{D_0} = 0.68$.

Critical Probe Length

One phenomenon of special interest in this study is the existence of critical probe geometries that distinguish fundamentally different flowfields. For a short probe, the flow separates from the probe and reattaches to the mainbody. As the probe is extended, there will be a length beyond which the flow reattaches to the probe sides, proceeds along the probe, and then separates again ahead of the mainbody. These two flows are essentially the same as the "open" and "closed" modes, respectively, of a cutout or cavity in a wall, as sketched in Fig. 11.[4,15–18,20] The probe length at which the flow changes from one mode to the other is defined as the critical length, which is a function of Mach number, Reynolds number, d_1/d_2, and the shape of the probe and mainbody corners. Some examples of both modes for different parameters are contained in the results presented in this paper.

An open-type flow is depicted in Fig. 12a for configuration 7 at $M = 0.91$, where the flow separates from the probe face and reattaches to the mainbody face. When this diameter probe is extended sufficiently, as shown in Fig. 12b for configuration 8 also at $M = 0.91$, the flow tends to reattach to the probe sides. The precise location of reattachment is not clear from this figure because the shadowgraph shows only details of the gross flow turbulence and because the outer boundary of this turbulent flow region does not coincide with the zero streamline or separation shear layer. The drag coefficient is somewhat higher for this closed-type flow. At slightly supersonic speeds, the distinction between open and closed modes for this diameter probe is much clearer. The open flow (Fig. 12c) has a bow shock, weak waves generated by turbulence in the free shear layer, and an oblique shock on the mainbody sides. In contrast, the closed flow (Fig. 12d) has, in addition to the waves of the open flow, two shocks on the probe sides. An oblique shock forms about one probe diameter downstream of the probe face, where the separated flow from the probe face reattaches. At approximately three probe diameters downstream of the probe face, another oblique shock forms and the flow separates from the probe sides. As with the subsonic case, the closed flow has slightly more drag than the open flow.

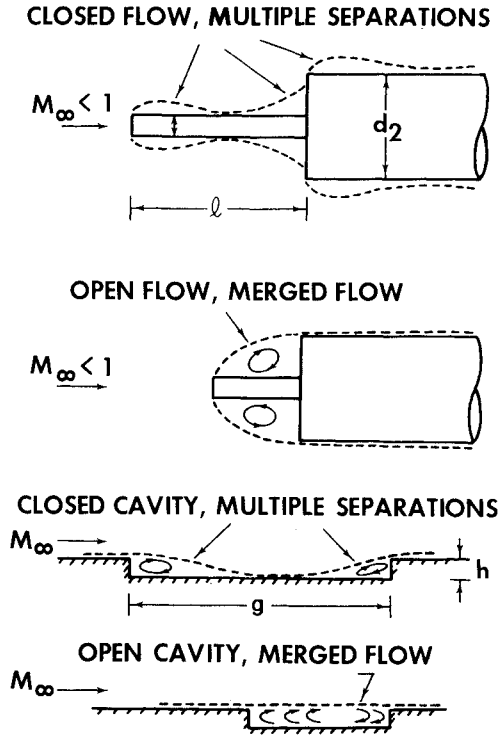

Fig. 11 Probe/cylinder flows with analogous cavity flows.

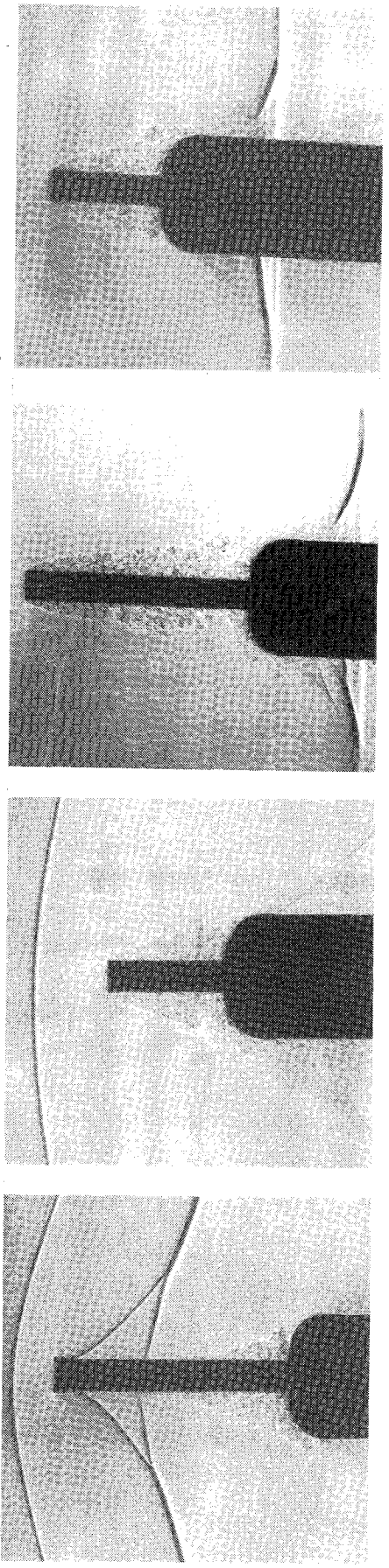

Fig. 12 Transonic open and closed flow: a) configuration 7, $\ell/d_2 = 0.96$, $d_1/d_2 = 0.248$, $M = 0.91$, $C_{D_0} = 0.47$; b) configuration 8, $\ell/d_2 = 1.92$, $d_1/d_2 = 0.248$, $M = 0.91$, $C_{D_0} = 0.50$; c) configuration 7, $\ell/d_2 = 0.96$, $d_1/d_2 = 0.248$, $M = 1.08$, $C_{D_0} = 0.70$; d) configuration 8, $\ell/d_2 = 1.92$, $d_1/d_2 = 0.248$, $M = 1.11$, $C_{D_0} = 0.80$.

Flow Oscillations

Previous investigators of geometries similar to the ones considered here have not consistently observed drag reductions when probes are used on blunt-nosed bodies at transonic speeds.[2,11,25] It has been suggested that large-scale oscillations of the probe or spike flow are responsible for creating net overpressures on the mainbody face and thus high drag.[11] Many of the situations explored in the present study also show evidence of flow oscillations. For example, Fig. 10 presents flows that are clearly unsteady, as indicated by the large number of spherical waves propagating away from the free shear layer. (These waves also appear in several of the other shadowgraphs.) The situation in Fig. 10 (configuration 5, $M = 0.95$) represents a configuration with less drag than its particular reference body (configuration 3), even in the transonic regime. Thus, it appears that the existence of flow oscillations does not necessarily lead to increased drag. Gharib[26] shows that axisymmetric cavity drag can be reduced when flow oscillations are present. Reference 6 also contains an example of an oscillating flow with lower drag than the same geometry without oscillations. Clearly, a very careful and extensive investigation is required before a proper relationship can be established between drag and flowfield oscillations.

Conclusions

This work has demonstrated that a potential exists for using probes as induced flow separation devices to reduce transonic blunt-body drag. For the best configuration encountered here, the reduction is 25% of the moderately blunt reference-body drag over the entire transonic regime. Based on experience with low subsonic and supersonic flows, the reduction can probably be improved with a careful parametric investigation of probe diameter and length.

The flowfield past these probe/cylinder geometries is characterized by flow separation from the probe face and eventual reattachment to the mainbody. For the lower-drag cases, there appears to be relatively smooth reattachment to the mainbody sides, whereas when the drag is higher, reattachment is more likely to occur at the mainbody face. The probe flowfield also exhibits various modes resembling those of open and closed cavity flows, depending primarily on the length of the probe. Short probes have a separation that reattaches to the mainbody much as an open cavity does. For longer probes, reattachment occurs at the probe sides, followed by a second separation near the mainbody face, as with a closed cavity. The geometrical and flow parameters determining which mode occurs are still to be determined. Unsteadiness on a large scale is an inherent feature of the flows seen here. However, the unsteadiness does not negate the effectiveness of the probe as a drag-reduction device.

The probe/cylinder geometries considered here are interesting not only for their possible applications as low-drag configurations but also for the wealth of information they can provide on flow separation and reattachment. The nature of the reattachment for low-drag, as opposed to high-drag, geometries; the conditions leading to closed or open cavity-like flow; and the nature and influence of the large-scale instabilities of the separated shear layer are among the more important questions that arise in the study of these probe/cylinder geometries. The present work has touched very briefly on each of these questions, but there is still much to be learned from investigations of combinations of axially aligned probes and cylinders in transonic flow.

References

[1]Mason, W. T. Jr. and Beebe, P. S., "The Drag Related Flow Field Characteristics of Trucks and Buses," *Proceedings of the Symposium on Aerodynamic Drag Mechanisms of Bluff Bodies and Road Vehicles*, edited by E. G. Sovran, T. Morel, and W. T. Mason Jr., Plenum, New York, 1978, pp. 45–93.

[2]French, N. J. and Jecmen, D. M., "Transonic/Supersonic Wind Tunnel Investigation of Effects of Parametric Variations in Nose Fair-

ing and Aerospike Geometry on Trident 1 C4 Missile Body Static Stability and Drag," Lockheed Missiles and Space Co., Sunnyvale, CA, LMSC-D 366908, Sept. 1974.

[3]Eaton, J. K. and Johnston, J. P., "A Review of Research on Subsonic Turbulent Flow Reattachment," *AIAA Journal*, Vol. 19, Sept. 1981, pp. 1093–1101.

[4]Roshko, A., "Some Measurements of Flow in a Rectangular Cutout," NACA, TN-3488, Aug. 1955.

[5]Morel, T. and Bohn, M., "Flow over Two Circular Disks in Tandem," *Journal of Fluids Engineering*, March 1980, pp. 104–111.

[6]Koenig, K., "Interference Effects on the Drag of Bluff Bodies in Tandem," Ph.D. Thesis, California Institute of Technology, Pasadena, University Microfilms, 1978.

[7]Koenig, K. and Roshko, A., "An Experimental Study of Geometrical Effects on the Drag and Flow Field of Two Bluff Bodies Separated by a Gap," *Journal of Fluid Mechanics*, Vol. 156, July 1985, pp. 167–204.

[8]Mair, W. A., "Experiments on Separation of Boundary Layers on Probes in Front of Blunt-Nosed Bodies in a Supersonic Air Stream," *Philosophical Magazine*, Ser. 7, Vol. 43, No. 342, July 1952, pp. 695–716.

[9]Beastall, D. and Turner, J., "The Effect of a Spike Protruding in Front of a Bluff Body at Supersonic Speeds," ARC R & M 3007, 1957.

[10]Album, H. H., "Regarding the Utility of Spiked Blunt Bodies," *Journal of Spacecraft and Rockets*, Vol. 5, Jan. 1968, pp. 112–114.

[11]Walchner, O. and Sawyer, F. M., "Effect of Nose Spikes on the Stability of Finless and Spinless Blunt Bodies in Free Supersonic Flight," Aeronautical Research Laboratory, Wright Patterson AFB, OH, ARL-TR 60-273, Aug. 1960.

[12]Zorea, C. and Rom, J., "Effect of a Spike on the Drag and on the Aerodynamic Stability of Blunt Bodies in Supersonic Flow," *Journal of Spacecraft and Rockets*, Vol. 7, Aug. 1970, pp. 1017–1019.

[13]Crawford, D. H., "Investigation of the Flow Over a Spiked-Nose Hemisphere-Cylinder at a Mach Number of 6.8," NASA TN D-118, Dec. 1959.

[14]Chapman, D. R., Kuehn, D. M., and Larson, H. K., "Investigation of Separated Flows in Supersonic and Subsonic Streams with Emphasis on the Effect of Transition," NACA TN-3869, March 1957.

[15]Johannesen, N. H., "Experiments on Supersonic Flow Past Bodies of Revolution with Annular Gaps of Rectangular Section," *Philosophical Magazine*, Ser. 7, Vol. 46, No. 372, Jan. 1955, pp. 31–39.

[16]Charwat, A. F., Roos, J. N., Dewey, F. C. Jr., and Hitz, J. A., "An Investigation of Separated Flows—Part 1: The Pressure Field," *Journal of Aerospace Sciences*, Vol. 28, June 1961, pp. 459–470.

[17]Rossiter, J. E., "Wind-Tunnel Experiments on the Flow Over Rectangular Cavities at Subsonic and Transonic Speeds," ARC R & M 3438, 1966.

[18]Wu, J. M. et al., "Fundamental Studies of Subsonic and Transonic Flow Separation: Part II—Second Phase Summary Report," University of Tennessee Space Institute, Tullahoma, TN, AEDC-TR-77-103, Dec. 1977.

[19]Spooner, S. H., "Static Longitudinal Stability Characteristics of a Series of 90-Millimeter Artillery Shells at Mach Numbers of 0.8, 0.9, 1.0 and 1.2," NACA RM-SL56D27, May 1956.

[20]Koenig, K., "Transonic Merging Separated Flows," Final Report, AFOSR Grant 83-0179, Mississippi State University, Starkville, MS, July 1984.

[21]Winchenbach, G., Galanos, S., Kleist, J., and Lucas, B., "Description and Capabilities of the Aeroballistic Research Facility," U.S. Air Force Armament Laboratory, Eglin AFB, FL, AFATL-TR-78-41, Feb. 1978.

[22]Whyte, R., Winchenbach, G., and Hathaway, W., "Subsonic Free Flight Data for a Complex Asymmetric Missile," *Journal of Guidance and Control*, Vol. 4, Jan.–Feb. 1981, p. 59.

[23]Stanbrook, A., "A Correlation of the Forebody Drag of Cylinders with Plane and Hemispherical Noses at Mach Numbers from Zero to 2.5," ARC CP 709, 1964.

[24]Rockwell, D. and Knisely, C., "The Organized Nature of Flow Impingement Upon a Corner," *Journal of Fluid Mechanics*, Vol. 93, Aug. 1979, pp. 413–432.

[25]Guenther R. A. and Reding, J. P., "Fluctuating Pressure Environment of a Drag Reduction Spike," AIAA Paper 77-90, Jan. 1977.

[26]Gharib, M., "The Effect of Flow Oscillations of Cavity Drag and a Technique for Their Control," Ph.D. Thesis, California Institute of Technology, Pasadena, University Microfilms, 1984.